

SIMPLE LOW-LOSS WAVEGUIDE BENDS USING ANTIRESONANT REFLECTING OPTICAL WAVEGUIDES

Marko Galarza¹, Jokin Moreno¹, Manuel López-Amo¹, Ilse Christiaens², Dries Van Thourhout² and Roel Baets²

¹ Electric and Electronic Department, Public University of Navarre, Campus of Arrosadia, 31006 Pamplona, Spain
marko.galarza@unavarra.es

² Department of Information Technology, University of Ghent-IMEC, St.-Pietersnieuwstraat 41, B-9000 Ghent, Belgium

SUMMARY

A new concept for reducing bend loss in dielectric planar waveguides based on antiresonant reflecting optical waveguides (ARROW) is presented. It has been ascertained by simulation that the bending loss can be significantly reduced.

KEYWORDS

Dielectric planar waveguides, bend waveguides, bend loss

ABSTRACT

INTRODUCTION

Curved waveguides are key components in photonic integrated circuits and are mainly used to change the direction of light or to introduce a lateral displacement. In order to achieve a high packing density in limited chip areas, it is mandatory to minimize the bend radius as much as possible, without introducing significant bend loss. Unfortunately, bend loss increases almost exponentially with decreasing radius of curvature.

There exist three major methods for reducing bend loss. One method is the introduction of refractive index changes in order to increase the relative index difference between the core and the cladding [1] or to accelerate the phase fronts at the outer side of the bend [2]. A second method replaces the bend by a coherently coupled multisection bend to reduce the loss [3]. The introduction of an isolation trench [4], corner mirror [5] or outrigger waveguide of higher refractive index [6] on the outside of the bent core decreases the evanescent modal field more rapidly in the region between the waveguide core and the apparent origin of radiation, so that radiation loss is also reduced. Nevertheless, most of these strategies involve additional processing steps during fabrication.

In this paper, we propose a novel and straightforward technique for reducing the bend radius by making use of ARROW (antiresonant reflecting optical waveguide) structures [7, 8]. The concept has the advantage that it does not require any extra processing step. A set of N concentric waveguides on the outer side of the bend and defined in the same step as the main waveguide (Fig. 1), are designed to provide antiresonant reflection to the radiated light. A ray radiated from the bend will undergo multiple reflections at each interface defined by the ARROW structure, and for an appropriate design the rays coming back to the curved waveguide have the same phase, interfering constructively and coupling back to the propagating mode. Fig. 1.a shows the electric field plot of light propagating in a bend of constant radius. We observe a huge power leakage for the bend mode. To the contrary, the corresponding ARROW curve with 4 lateral waveguides of Fig. 1.b shows almost no power leakage to the outside of the bend.

INP RIB WAVEGUIDE

For the simulations, we assume in a first example a typical InP/InGaAsP low confinement rib structure consisting of a quaternary core layer of refractive index n_{co} and thickness h_{co} on an InP substrate and with a top InP cladding layer with a thickness h_{cl} . The waveguide has a width w and is etched down to the top of the quaternary layer. The N lateral rib waveguides, structurally identical to the main waveguide, are also shown in Fig. 2. Each of them is w_l wide and is separated by a distance d_l from the previous rib.

A commercial 3-D complex mode solver (Fimmwave) [9] was used to design the optimal dimensions for the lateral ARROW waveguides and quantify the improvement achieved. The fully vectorial mode solver is based

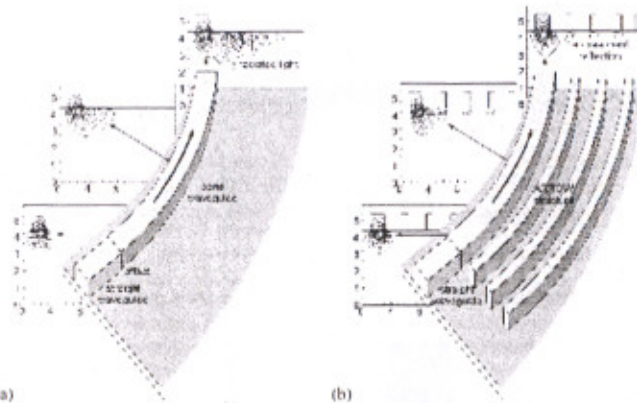


Figure 1. Schematic drawing of the proposed bend concept. (a) Propagation field in a standard bend waveguide; (b) propagation field along the same waveguide bend having lateral ARROW waveguides.

on the film mode matching method [10], which, in the case of curved waveguides, solves the Maxwell equations in cylindrical coordinates. A perfectly matched layer (PML) located at the outer side of the bend absorbs the power leaked out of the bend, avoiding any parasitic reflection, thanks to the imaginary part of its thickness. Since no radiation is produced towards the other three transverse directions in the low confinement rib waveguide considered, perfect electric (PEC) and magnetic (PMC) conductors are used as boundary conditions for these. With this scheme the mode solver allows to calculate the losses of the different modes and their propagation constants.

For each lateral rib two parameters have to be defined: its width w_i and the gap d_i . The N ARROW waveguides were sequentially optimized by scanning for the minimum loss point in the 2D parameter space (w_i, d_i). We consider a waveguide of width $w = 3 \mu\text{m}$, a core with index $n_{co} = 3.36$ (Q1.25) and thickness $h_{co} = 600 \text{ nm}$, a cladding and substrate index $n_{cl} = 3.17$, a cladding thickness $h_{cl} = 300 \text{ nm}$, and an excitation wavelength of $\lambda = 1.55 \mu\text{m}$ for the analysis. Fig. 3 shows the bending loss, in dB/90°, as a function of the width w_i of each lateral waveguide, for a radius of $500 \mu\text{m}$ and for TE polarization. For each rib the choice of d_i corresponds to minimum bend loss. As shown we considered $N = 6$ lateral waveguides.

A quasi-periodic Fabry-Pérot-like response, typical for antiresonant reflecting structures, is obtained. Circles surrounding the minimum loss points for the first periods represent the starting points for the consecutive scans. In each step, a significant loss reduction is obtained. A slight reduction of the oscillation is observed for

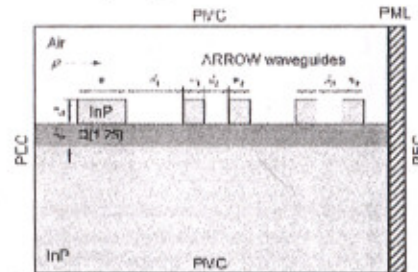


Figure 2. Cross-section of the InP ARROW bend waveguide and detail of the boundaries used in the simulation: PEC and PMC stand for perfect electric and magnetic conductors, respectively; PML is a perfectly matched layer, which absorbs the radiation in the bend.

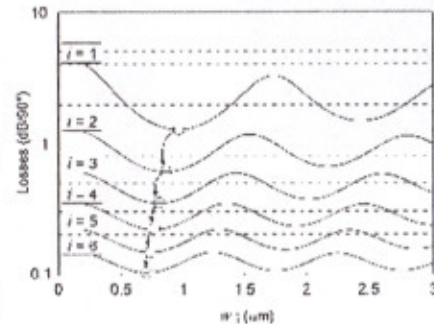


Figure 3. Bending loss as a function of the width w_i of each of the $N = 6$ lateral waveguides. The first minimum of the quasi-periodic response is used in the sequential design. The choice of d_i corresponds to minimum bend loss.

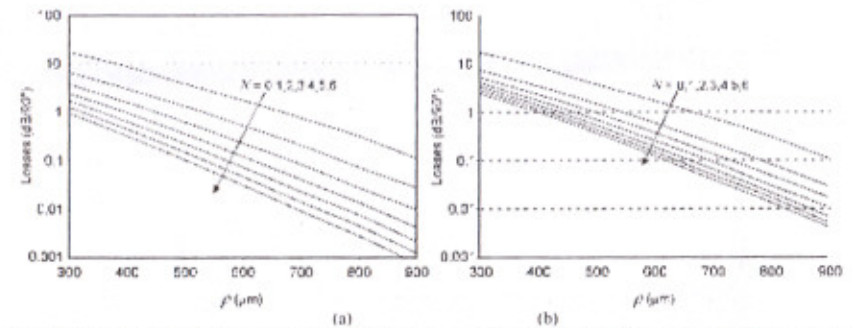


Figure 4. Bending loss per 90° as a function of bend radius and number of lateral waveguides N for (a) first minimum, and (b) second minimum working point designs.

successive periods due to the decrease of the radial component of the wave number with the radius [11]. The optimal rib widths w_i and the gaps d_i decrease with decreasing radius, and most calculated dimensions are sub-micrometer, even for the biggest radius $\rho = 900 \mu\text{m}$. Such small features may be difficult to achieve with standard photolithography. However, taking into account the periodicity of the Fabry-Pérot like response of the ARROW structure we can shift the working point to the minimum of the second period in order to increase the minimum waveguide features. The minimum feature, for the smallest radius, is now $0.9 \mu\text{m}$, while the rest are higher than $1 \mu\text{m}$, perfectly achievable with standard lithographic techniques.

Fig. 4 shows the calculated radiation losses of the waveguide, as a function of bending radius ρ and for different numbers N of lateral ARROW waveguides for the first (Fig. 4.a) and second (Fig. 4.b) minimum point designs. In the former, the loss in dB is reduced by a factor of 10 using only 3 lateral ribs, and keeps on decreasing significantly using the other 3 ribs. The improvement factor is higher for big radii than for small ones. From an integration point of view, we observe that for a given loss, it is possible to reduce the radius of the bend by a factor close to 2, which means that the area can be reduced by a factor close to 4. By increasing the number of ribs further, the area reduction ratio could still be increased.

From the results provided by the second minimum design (Fig. 4.b), we see a lower improvement compared to the previous structure. A loss reduction factor higher than 10 dB for a given radius was achieved using all the 6 lateral ribs. Also here, increasing the number of lateral ARROW waveguides will lead to additional loss reduction.

As mentioned above, the simulated designs were optimized for TE polarization. Due to the fact that the waveguide is shallowly etched, TM polarization presents lower radiation losses than the minimum obtained for TE in any of the two ARROW bend structures and even in the standard bend, making them polarization independent.

SILICA BURIED WAVEGUIDE

As a second example we consider a silica-on-silicon waveguide with core refractive index $n_{co} = 1.4550$, cladding index $n_{cl} = 1.4442$ ($\Delta = 0.75\%$), core width and height $w = 5.5 \mu\text{m}$, and operating wavelength $\lambda = 1.55 \mu\text{m}$ (see Fig. 5). The main disadvantage of silica-on-silicon technology is the required high bending radius due to a low index contrast. Perfectly matched layers have been located at the indicated three sides of the bend in order to absorb all of the power leaking out of the buried bend.

Fig. 6 shows the calculated bending losses of this new waveguide structure as a function of bending radius ρ and number of lateral ribs N for TE polarization. A higher number of lateral waveguides are needed to reduce the radiation losses compared with the InP technology, but the minimum features w_i and d_i are all bigger than $1 \mu\text{m}$. And naturally, there is no a priori limitation on the number of lateral buried waveguides that can be defined at the outer side of the bend. Therefore, it would be possible to reduce optical power leakage further by just defining more than 6 lateral ribs. It is believed that the poor improvement for the last two lateral waveguides and for big radii is due to the proximity of the outer PML layer to these waveguides in the utilized window. Similar design and loss curves are obtained for TM polarization demonstrating polarization independent performance in silica technology.

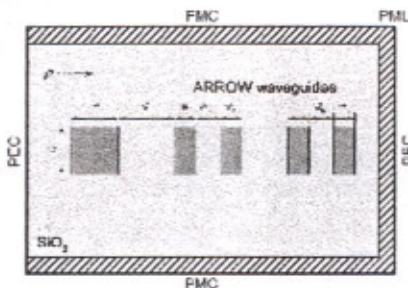


Figure 5. Cross-section of the silica ARROW bend waveguide and detail of the boundaries used in the simulation.

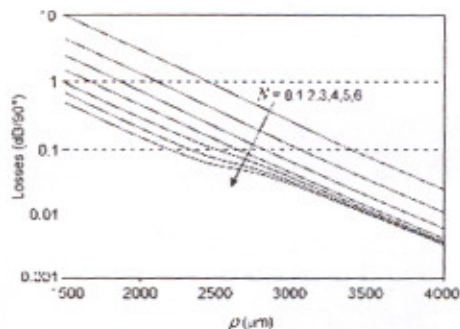


Figure 6. Bending loss per 90° as a function of bend radius and number of lateral waveguides N for the silica waveguide.

FABRICATION TOLERANCES

The performance of ARROW bends as a function of variations in the width of the lateral ribs has also been studied. It is very common to have this kind of variations during the processing of the devices. We have calculated the radiation losses of the two proposed ARROW bend structures (designed around the $0.1 \text{ dB}/90^\circ$ loss working point and having $N = 6$ lateral ribs) as a function of a general variation in the widths of the lateral ribs. We have observed a smooth increase of the loss by less than 1 dB in a safe lithographic range (width varies by $\pm 350 \text{ nm}$) for both technologies.

CONCLUSION

We have proposed and analyzed a new bend concept based on the ARROW effect which is provided by a set of properly designed waveguides. These waveguides are defined in the same processing step as the central bend waveguide, and thus, do not require any additional processing. Applicability to typical InP and Si-based waveguide structures has been analyzed and a significant bending-loss reduction has been observed. The concept is compatible with other bending-loss reduction techniques using one photolithographic step, such as S-shaped bends, continuous waveguide widening and bending, and even with multisectional bends [3], as well as with most of the transition loss reduction techniques.

ACKNOWLEDGMENTS

This work was supported by European Sixth Framework Programme under a Marie Curie grant, and Ministerio Español de Ciencia y Tecnología under projects TIC2001-0877-C02-02 and TEC2004-05936-C02-01

REFERENCES

- 1) R. A. Jarvis, J. D. Love, F. Ladouceur: *Electron. Lett.* **33**, 892–894 (1997).
- 2) S. Tomljenovic-Hanic, J. D. Love, A. Ankiewicz: *Electron. Lett.* **38**, 220–222 (2002).
- 3) J.-J. Su, W.-S. Wang: *IEEE Photon. Technol. Lett.* **14**, 1112–1114 (2002).
- 4) C. Seo, J. C. Chen: *J. Lightwave Technol.* **14**, 2255–2259 (1996).
- 5) L. H. Spiekman, Y. S. Oei, E. G. Metaal, F. H. Groen, P. Demeester, M. K. Smit: *IEE Proc.-Optoelectron.* **142**, 61–65 (1995).
- 6) S. N. Radcliffe, T. P. Young: *IEEE J. Select. Area. Commun.* **6**, 1169–1177 (1988).
- 7) M. A. Duguay, Y. Kokubun, T. L. Koch, L. Pfeiffer: *Appl. Phys. Lett.* **49**, 13–15 (1986).
- 8) T. Baba, Y. Kokubun: *IEEE Photon Technol. Lett.* **1**, 232–234 (1989)
- 9) Fimmwave, Photon Design; <http://www.photonod.com>
- 10) A. S. Sudbo: *IEEE Photon. Technol. Lett.* **5**, 342–344 (1993).
- 11) E.C.M. Pennings: PhD Thesis, ISBN 90-9003413-7 (1990).



OWTNM 2005

Grenoble ~ France

Optical Waveguide Theory and Numerical Modelling

13th International workshop
April 8-9 2005, Grenoble, France

Proceedings

OWTNM'05 Program

Thursday April 7 2005

17 : 00 – 18 : 30 Registration (Atrium)

Friday April 8 2005

08 : 00 Registration (Atrium)

08 : 30 Plenary session (Auditorium)

Session FrP1 (joint with ECIO'05) Tutorials **Chair:**

08 : 30

Andrea Fiore, EPFL, Lausanne, Switzerland

Quantum dots for optical applications

09 : 15

Pierre Viktorovitch, LEOM, Ecole Centrale de Lyon, France

Photonic Crystals : basic concepts and applications

09 : 45 Coffee break

10 : 15 Modelling of integrated and nanophotonics devices I (Makalu room)

Session FrB1 (joint with ECIO'05) **Chair: I. O'Connor**

10 : 15

FrB1-1 (Invited: paper): Efstathios D. Kyriakis-Bitzaros, Institute of Microelectronics, NCSR "Demokritos", Greece

System level modelling and simulation of optical interconnects

10 : 45

FrB1-2 : Emmanuel Drouard, Matthieu Brière, Andrzej Kazmierczak, Xavier Letartre, Ian O'Connor, and Frédéric Gaffiot, LEOM, Ecole Centrale de Lyon, France

Phenomenological modelling of WDM crossbars based on channel drop filters

11 : 00

FrB1-3 : Laurence Cahill, La Trobe University, Melbourne, Australia

Approximate analysis of cascaded generalised Mach-Zender switches

11 : 15

FrB1-4 : Pablo Sanchis, Javier Martí, Jaime Garcia, Universidad Politécnica de Valencia, Valencia, Spain

Peter Bienstman and **Roel Baets**, Ghent University, IMEC, Gent, Belgium

Semi-analytic analysis of complex photonic crystal structures

11 : 30

FrB1-5 : M.J.R. Heck1, E.A.J.M. Bente, D. Lenstra, M.K. Smit, Y. Barbarin, Technische Universiteit Eindhoven, Eindhoven, The Netherlands
P. Muñoz, iTEAM Research Institute, Universidad Politecnica de Valencia, Spain

Simulation and design of integrated pulse shaping components for femtosecond modelocked ring lasers

11 : 45

FrB1-6 : C. Xing, E.A. Avrutin, University of York, York, UK
Theory of monolithically integrated actively mode-locked quantum dot lasers

12 : 15 Lunch

13 : 30 Modelling of integrated and nanophotonics devices II (Makalu room)

Session FrB2 (joint with ECIO'05)

Chair: Ivo Montrosset

13 : 30

FrB2-1 (Invited: paper): Jiri Ctyroky, Institute of Radio Engineering and Electronics Prague, Czech Republic

Modelling of guided-wave optical microresonators

14 : 00

FrB2-2 : Kirankumar R. Hiremath, Manfred Hammer, University of Twente, Enschede, The Netherlands
Perturbational evaluation of bend mode phase shifts for the tuning of cylindrical microresonators

14 : 15

FrB2-3 : Marko Galarza, Jokin Moreno, Manuel López-Amo, Public University of Navarre, Pamplona, Spain

Ilse Christiaens, Dries Van Thourhout and Roel Baets, University of Ghent-IMEC, Ghent, Belgium
Simple low-loss waveguide bends using antiresonant reflecting optical waveguides

14 : 30

FrB2-4 : Remco Stoffer, Phoenix BV, Enschede, The Netherlands

Kirankumar R. Hiremath, Manfred Hammer, MESA+, University of Twente, Enschede, The Netherlands
Ladislav Prkna, Laboratoire de Photonique et de Nanostructures, CNRS, Marcoussis, France
Jiri Ctyroky, Institute of Radio Engineering and Electronics, Czech Academy of Sciences, Prague, Czech Republic

Simulations of vertically-coupled microdisk-resonators by 3-D vectorial coupled mode theory

14 : 45

FrB2-5 : Dongwoo Suh, Yongwoo Park, Yeungjoon Sohn, Hesuk Jung, Mun Cheol Paek, Kwangyong Kang, Electronics and Telecommunications Research Institute, Republic of Korea

Optimization of leaky mode directional coupler for the application to a small form factor disk pickup

15 : 00 Waveguides and devices (Makalu room)

Session Fr3

Chair:

15 : 00

Fr3-1 : Marco Gnan, A. R. Md Zain, H. M. H. Chong, R. M. De La Rue, University of Glasgow, Glasgow, United Kingdom

Modelling of Photonic Wire Bragg-Grating Structures

15 : 15

Fr3-2 : **Y Zhang**, T M Benson, P Sewell, D Zhang, W Pan, D Furniss and A B Seddon, University of Nottingham, Nottingham, United Kingdom

The Design of Glass-Based Waveguides for Photonic Integrated Circuits

15 : 30

Fr3-3 : **F.P. Payne**, University of Oxford, United Kingdom

An Accurate Analytical Solution for the Coupling Between the Array Waveguides in AWGs and Star Couplers

15 : 45

Fr3-4 : **Stefano Beri**, Mirvais Yousefi, Piet C. De Jagher, Meint Smit, Daan Lenstra, COBRA, Eindhoven University of Technology, The Netherlands

Modeling the coupling strength between two closely grown parallel ridge waveguides

16 : 00

Fr3-5 : **Y. X. Huang**, Y. Y. Lu, City University of Hong Kong, Kowloon, Hong Kong

Semi-vector Modeling of Waveguide Discontinuities

16 : 15

FR3-6 : **F. Riboli**, N.Daldosso, L.Pavesi, Trento University ,Physics Dep., Trento, Italy

G. Pucker, A.Lui, ITC-IRST, Microsystem Division, Povo-Trento, Italy.

Integrated in-line optical switch based on liquid crystal infiltration.

16 : 30

Fr3-7 : **J.D. Love**, A.W. Molloy and A. Ankiewicz, Optical Sciences Group, Australian National University, Canberra, Australia

Compact Geometrical 3-Wavelength Planar CWDM Devices

16 : 45

Fr3-8 : **Kien Phan Huy**, Alain Morand and Pierre Benech, IMEP, INPG-UJF-CNRS, Grenoble, France

High efficiency design WGM cavity using the Floquet-Bloch formalism

17 : 00 Coffee break

17 : 15 – 19 : 15 Poster session (Mont Blanc rooms)

(see "poster presentation").

20 : 00 Workshop dinner